

A NOVEL CW RFQ FOR EXOTIC AND STABLE BEAMS

A. Palmieri, L. Bellan, M. Comunian, L. Ferrari, C. Roncolato, A. Pisent
INFN-LNL, Legnaro (PD), Italy

Abstract

Meaning of a and b

The SPES RFQ is designed in order to accelerate beams in CW with A/q ratios from 3 to 7 from the Charge Breeder through the MRMS and the selection and injection lines up to the MEBT (Medium Energy Beam Transport). The RFQ is composed of 6 modules about 1.2 m long each. Each module is basically composed of a Stainless Steel Tank and four OFE Copper Electrodes. A copper layer is plated on the tank inner surface and a spring joint between tank and electrode is used in order to seal the RF. In this contribution, the main design steps of the RFQ, the construction concepts and the results obtained for the first assembled modules are shown.

ent configurations maximizes the RNB efficiency but needs a CW post accelerator (RFQ and ALPI). The beam is prepared for the post-accelerator stage with a charge breeder device (an ECR that works in continuous). The energy from 20 to 40 keV on the transfer lines are determined by the chosen RFQ input energy (5.7 keV/u); for this reason, all the devices where the beam is approximately stopped (production target, charge breeder and RFQ cooler) lay at a voltage proportional to the ratio A/q . The charge state range ($3.5 < A/q < 7$) is bounded by the RFQ field level for the upper limit and by the minimum voltage on $q=1$ transport line [1].

INTRODUCTION

SPES, acronym of Selective Production of Exotic Species, is a CW radioactive ion beam facility under construction at LNL INFN in Italy, aimed at the production and acceleration of neutron-rich radioactive ions, in order to perform nuclear physics experiments, which will require beams above Coulomb barrier [1]. The main functional steps of the facility are shown in Figure 1: the primary beam delivered by the cyclotron, the beam from the fission target (as an example, up to 10^{13} particle/s of ^{132}Sn), the beam cooler, the separators, the charge breeder and the accelerator (the existing ALPI with a new RFQ injector). The use of the continuous beam from the +1 source, which can use differ-

RFQ MAIN PARAMETERS AND BEAM DYNAMICS CHOICES

The RFQ (see Table 1) operates in a CW mode (100% duty factor) at a frequency of 80 MHz. This frequency is the same of the lowest energy ALPI superconducting structures. The SPES RFQ is provided with internal bunching, in order to improve beam transmission. The injection energy of ions is set to 5.7 keV/u. This choice is aimed at getting more cells at low energy i.e. low output longitudinal emittance. The extraction energy was set to 727 keV/u (respect to the 588 keV/u of the present super-conducting RFQ, named "PIAVE"), in order to optimize the beam dynamics of the SRF ALPI linac (see Table 1).

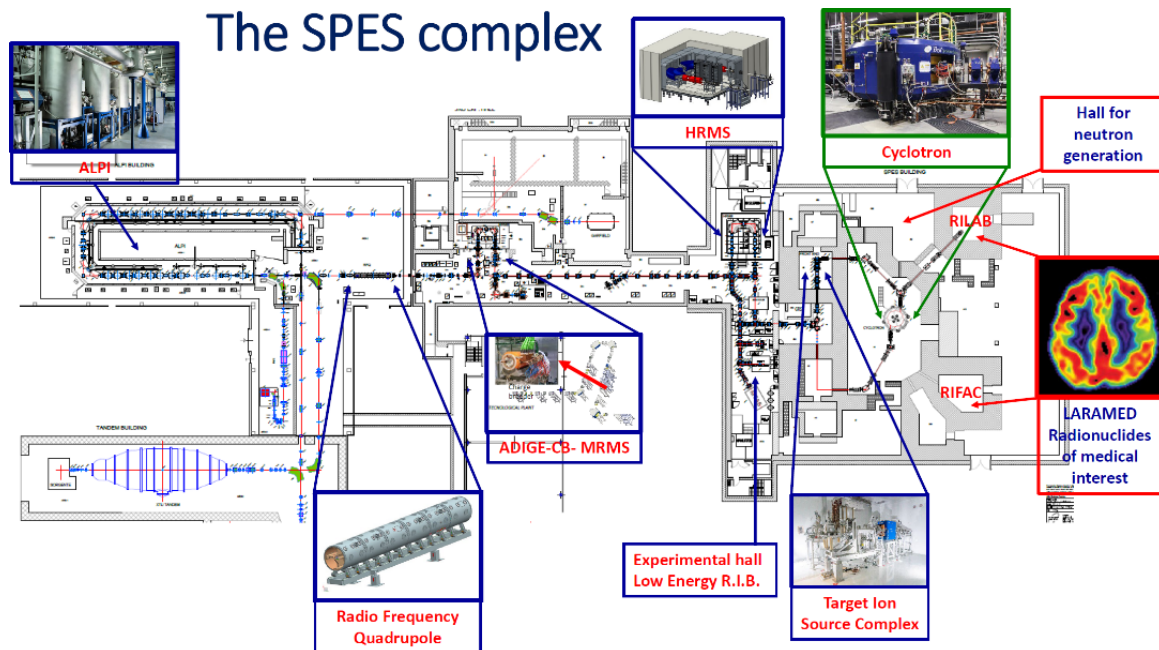


Figure 1: General SPES layout with main areas.

Table 1: Principal RFQ Parameters

Parameter (units)	Value
Operational mode	CW
Frequency	[MHz] 80
Injection Energy	[keV/u] 5.7 ($\beta=0.0035$)
Output Energy	[keV/u] 727 ($\beta=0.0395$)
Accelerated beam current	[μ A] 100
Charge states of accelerated ions [Q/A]	7-3

For the given input conditions, the main beam dynamics choices were aimed at minimizing the longitudinal and transverse emittance growths and to optimize the RF losses (<150 kW in order to take advantage of the available amplifier technologies) and transmission of the RFQ structure with the goal of a surface electric field below 1.8 Kilp. The RFQ cells were created using a home-made routine, based on the program used for the design of CERN linac3 RFQ, while the multiparticle transport was performed by PARMTEQM code package and TraceWin/Toutatis. With this design the RF power consumption is minimized, while a linear voltage profile allows accelerating the beam more effectively at higher velocities and achieving a shorter RFQ. A transition cell was used at both the entrance and exit of the RFQ. Table 2, Fig. 1 and Fig. 2 show the main parameters of the RFQ. The RFQ transmission is more than 95% of accelerated particles, the final longitudinal RMS emittance is 0.15 ns·keV/u (4.35 deg·keV/u). The 99% longitudinal emittance is 1.2 ns·keV/u. In Table 2 the main RFQ parameters as per Beam Dynamics Optimizations are shown, while in Figure 2 some of these parameters are shown as they evolve along the RFQ length.

Table 2: RFQ Design Parameters

Parameter (units)	Value
Inter-Vane Voltage [kV] ($A/q=7$)	63.81–85.84
Vane Length L [m]	6.95
Average Radius R_0 [mm]	5.33–6.79
Vane Radius ρ to average Radius ratio	0.76
Modulation Factor m	1.0/3.18
Minimum aperture a [mm]	2.45
Total number of Cells	321
Synchronous Phase [$^\circ$]	$-90^\circ / -20^\circ$
Focusing Strength B	4.7/4
Surface E field [kilp.]	1.74
Transmission [%]	95
Input Tr. RMS Emittance [mm·mrad]	0.1
Output Longitudinal RMS Emittance [keV·deg/u]/[ns·keV/u]	4.35/0.15

The RFQ performances were verified as well by performing a set of error studies, covering the input beam current variation (0 to 1 mA), input emittance (0.1 to 0.5π -mm·mrad), RFQ voltage ($\pm 6\%$ range), tuning errors

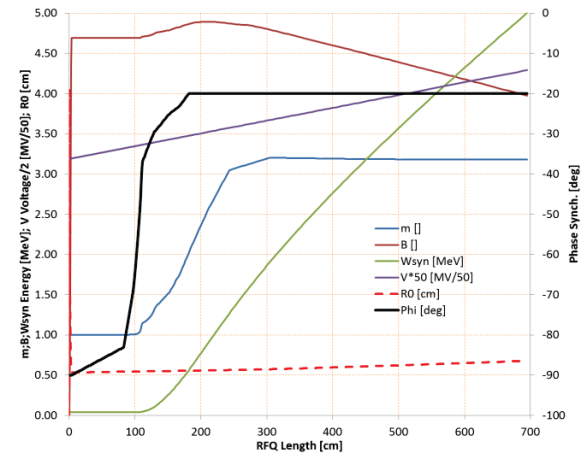


Figure 2: Main RFQ parameters vs length.

(i.e. voltage tilt and harmonic perturbations superimposed to the nominal law), and electrode displacement. As a conclusion, the RFQ keeps its transmission drop below 0.5% with respect to the nominal value and longitudinal emittance growth below 2,5% as far as the voltage variations and/or tilts are kept below $\pm 3\%$, which is, ultimately, the goal of the RFQ tuning.

Figure 3 shows the phase and the radial amplitude particle density along the RFQ, the plot is obtained from a Toutatis multiparticle simulation [2].

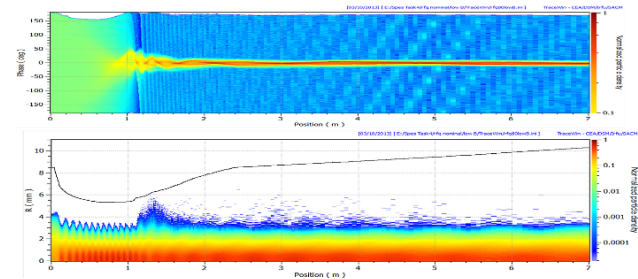


Figure 3: Phase and Radial density amplitude along the RFQ.

RFQ CAVITY DESIGN

The voltage law $V(z) = V(0) + b \cdot z$ with $b = 3.177$ kV/m and $V(0)$ depending on the A/q of the ion to be accelerated is obtained by proper shaping of the vane undercuts at both ends of the RFQ, by keeping the local TE_{21} cut-off frequency constant along z . Therefore, it was chosen to compensate the R_0 and ρ variations by capacitive tuning, by keeping the electrode thickness constant at 48 mm as well the angles $\alpha^1 = \alpha^2 = 30^\circ$, and the Tank radius $R = 377$ mm by varying the Y^4 parameter (Fig. 4).

The dimensioning of the vane undercut is made with a 45° angle and a tuning ring, machined on the end-plate (inner radius 150 mm, external radius 300 mm, thickness 0÷50 mm) is used for further tuning of the slope. The dimensions of the undercuts were optimized with HFSS simulations.

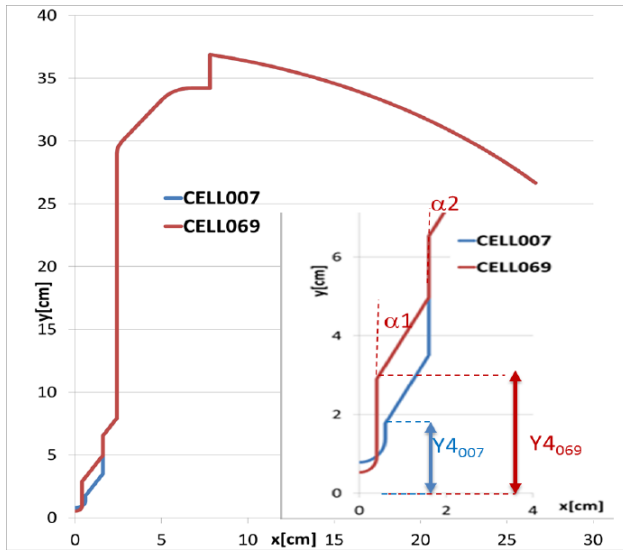


Figure 4: Capacitive tuning of the RFQ sections: maximum R_0 (blue curve) and minimum R_0 (red curve).

As it will explained in some detail later, in this RFQ the electrodes are assembled with the tank. Therefore, in order to allow proper operation of the RFQ, a RF joint must be placed longitudinally between the electrode and the tank. In addition, electrical properties of the joint have to comply with the possibility of ± 0.2 mm regulation of the electrode orthogonally with respect to beam axis. For this reason it was decided to use a multi-louver reed-shaped spring joint Contact louvers in copper, silver-plated and mounted on a stainless steel carrier, i.e. the LA-CUD/0,15 joint, by Multi-Contact® (400 louvers/m), which guarantees (in particular the LA-CUD joint) a current capability of tenth of Amperes per louver, the required regulation (± 0.6 mm, nominal), and a shrinkage force in the range of $(200\div 320)$ kg·m⁻¹ of spring joint. The variation of this force, connected with the positioning of the electrode, causes the contact resistance to vary accordingly (Fig. 5).

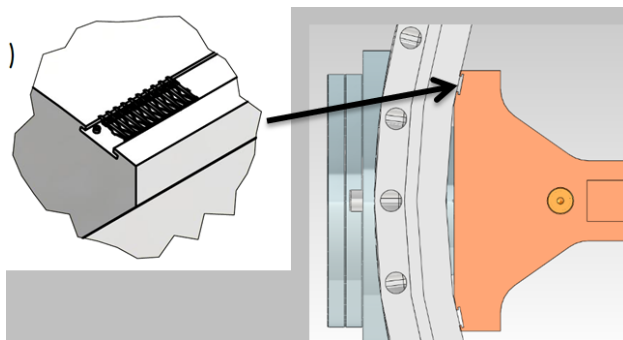


Figure 5: The RFQ electrode and the groove for the RF joint.

As for frequency sensitivities is concerned, it results that $\chi_{R_0} = \partial f / \partial R_0$ varies from 2.5 MHz/mm to 3.7 MHz/mm (average value 3.3 MHz/mm) and $\chi_R = \partial f / \partial R = -0.2$ MHz/mm. The frequency shift can be calculated as $\Delta f = \chi_{R_0} \Delta R_0 + \chi_R \Delta R \approx \chi_{R_0} \Delta R_0$ (in most cases the second term can be neglected). The number of tuners is $N_T = 68$ (17 per quadrant)

plus 3 extra tuners located at coupler position. The tuner radius is 59 mm the average tuner sensitivity is equal to about $\chi_{\text{tun}} = 13$ kHz/mm (all tuners). Therefore, the tuning range can be spanned with a range of tuner depths $h_t = [h_{\text{min}}, h_{\text{max}}] = [-10 \text{ mm}, 80 \text{ mm}]$, corresponding to a nominal tuner position of $h_0 = 35$ mm). In this case the tuning range of 1150 kHz, corresponds to frequency range of [79.39 MHz, 80.54 MHz] and a ΔR_0 range of ± 0.175 mm along all the RFQ, approximately equal to the electrode regulation range. The RF dissipated power value is equal to about 100 kW (with 30% margin for 3D details and RF joint), and, including a further 20% margin for LLRF regulation, the RF power is about 120 kW. In Table 3, the main RF parameters are shown.

Table 3: RFQ RF main Parameters (rated for $A/q=7$)

Parameter (units)	Value
Operational mode	CW
Frequency [MHz]	80
TE ₂₁ [TE ₁₁] cut-off frequency [MHz]	79.5 [77.3]
Q ₀ value	14000
Shunt Impedance times length [kΩ·m]	349–365
Dissipated Power in the cavity [kW]	100
RF power [kW]	120
Stored Energy [J]	2.87
Maximum Power density in the cavity sections [W/cm ²]	0.31
Maximum Power density in the cavity undercuts [W/cm ²]	11

Finally, the whole length RFQ (included modulation) underwent a combined ANSYS-HFSS RF and thermo-structural simulation. In Fig. 6 the vane voltage V calculated in some RFQ sections with the Faraday-Neumann law is shown in different cases, showing an agreement within $\pm 4\%$. This value (not yet tuned) can be considered as a validation of the RF design [3]. One interesting thing to be noticed is that the modulation made the Dipole-free region symmetric with respect to $f_{\text{TE}21} = 79.5$ MHz. This symmetry is due to the fact that modulation has a little effect (less than 200 kHz) on Q modes and D modes with order >0 but shifts of 1 MHz lower in frequency the TE₁₁ mode. Therefore, the RFQ is intrinsically «dipole free» and dipole rods are not needed [4].

RFQ ENGINEERING

Thermal Considerations

The RFQ Cooling System is designed to remove power and to finely tune the cavity resonant frequency during operation by temperature regulation. For such a purpose, it is necessary to have two independent water loops with two temperature set points: a “cold” circuit for the tank, end plates, the vacuum grids, the coupler and the tuners and a “warm” one for the vanes. By mixing with a 3-way valve the cold inlet water with part of the warm water coming from

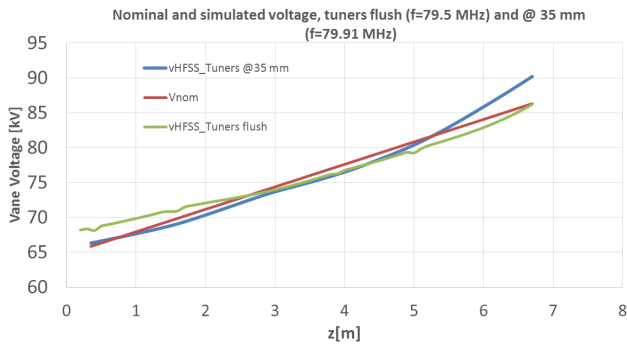


Figure 6: The RFQ voltage: nominal (red curve), tuner flush simulated (green curve), tuners at $h_{t0} = 35$ mm (blue curve). The simulation was performed on $\frac{1}{4}$ RFQ with 3 million mesh elements.

the cavity, it is possible to vary the resonant frequency of the RFQ and to tune the cavity accordingly. Let us observe that the vane and the tank are thermally insulated and that the RF power balance is approximately 60% on the vanes (Cu) and 40% on the tank (SS). The channel radii are $R_{c2} = 6$ mm on the vane and $R_{c1} = 4$ mm on the tank, the inlet water velocity is 2 m/s for the vane and 1.5 m/s for the tank. The reference inlet water temperatures are 15 °C for the tank and 20 °C for the vane. The cooling channel layout for the electrodes is shown in Fig. 7 [5].

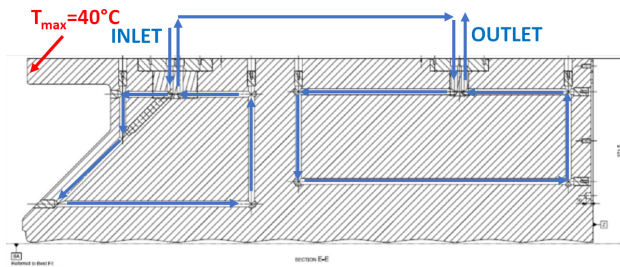


Figure 7: Cooling channel arrangement for the RFQ (case of high energy RFQ end).

In this case the water temperature increase is, in average, 2.6 °C, and the pressure drop is about 2 bars. The maximum temperature is about 40 °C and is reached in the upper part of the High Energy end undercut. As for the tank, there are 16 cooling channels, and the water temperature increase is 1.3 °C, while the maximum temperature of 47 °C occurs in the flange zone is higher, since the reduced thickness reduces heat conduction. In any case, the associated tip deformations are everywhere less than 20 μ m, with an overall effect on frequency less than 10 kHz. These results were obtained with a whole length RFQ (included modulation) combined ANSYS-HFSS RF and thermo-structural simulation. The vane temperature coefficient $\frac{\partial f}{\partial T_2}$ is equal to about -17 kHz/°C. Moreover, the frequency shift $\Delta f_{\text{on-off}}$ from maximum input power to zero input power is +85 kHz, and the vane + tank (isotropic) temperature coefficient $\frac{\partial f}{\partial T_{1,2}}$ (that is the frequency shift due to both T_1 and T_2 increase is -2 kHz/°C. Therefore, a temperature tuning range of about ± 85 kHz can be established for a T_2 variation in the range [15 °C, 25 °C]. Moreover, as power increases frequency in-

creases, as well as water temperature. Nevertheless, since $\frac{\partial f}{\partial T_{1,2}} < 0$, then a stabilizing mechanism is established, and a thermal runaway is avoided.

Mechanical Assembly Considerations

The RFQ is composed of 6 modules about 1.2 m long each. Each module is basically composed of an AISI 304 L SS Tank and four OFE Copper Electrodes (obtained by a single brazing cycle to avoid softening of the base material). A copper layer is plated on the tank inner surface and a spring joint between tank and electrode is used in order to seal the RF. Since the R_0 final values are determined by the electrode vs. tank positioning, the mechanical design and assembly procedure of the RFQ is aimed at obtaining both a precise and reliable assembly of the electrodes on the tank, as well as an accurate alignment of each RFQ module. For this reason, one can take advantage of the experience gained in IFMIF [6] project, by including some innovative elements in terms of the cavity assembly procedure.

The basic idea underlying the assembly procedure is to avoid on one hand large and/or not-round gasket mounting and on the other hand to decouple vacuum sealing and RF joints mounting, by avoiding simultaneous stresses on the components. For this reason, the interface joining the Electrode (EL) to the Tank (T) (Fig. 8) is made of two SS316LN Stainless Steel inserts, brazed on the electrode, on which cooling channel tube housings are placed, as well as an energized C-seal for vacuum sealing. The RF joints are to be contemporarily pushed against the inner tank surface with an overall max 8 kN force (8 N/louver) on the whole electrode length (2 RF joints/electrode). Indeed, each of the spring C-seal, needs 60 kN (167 N/mm on the circumference) for tightening, concentrated in the gasket diameter. Now, since the contemporarily tightening of the two C-seals would not be not feasible, the assembly interface was modelled in order to avoid dangerous stresses on the electrode, by making the assembly of one insert independent on the assembly of the other one. The Support Flange (SF) made of 316LN has the seats for two small gaskets and through holes (SF) for screws and cooling pipes. The external support flange hole pattern is in vacuum and will be enclosed in a donut-shaped Vacuum Cap (VC) via both an inner and an outer gasket. The stop surface in SF with the tank has to be machined according with mechanical/RF measurements to be performed in situ, in order both to avoid electrode deformations and proper electrode positioning with respect to tank axis. The Vacuum Cap (VC) has to guarantee vacuum tightness. Moreover, due to its relatively thin (1.5 mm) surface, it avoids stresses that could be induced by the non-parallelism of the two gasket stop surfaces. Finally, the Aluminium Extractor (EX) is such to house the SF, to tighten the RF joint, and to pull the electrode, as well as to allow the alignment pin insertion/extraction (Fig. 8). This setup was successfully prototyped before being employed as per brazing interface validation and the functionality of all the components, as well as determining possible issues in the electrode-vs-tank alignment assembly, via the usage of an

Content from this work may be used under the terms of the CC BY 4.0 licence (© 2022). Any distribution of this work must maintain attribution to the author(s), title of the work, publisher, and DOI

electrode simulacre with two inserts [3]. All the RFQ sealings are performed via spring energized gaskets.

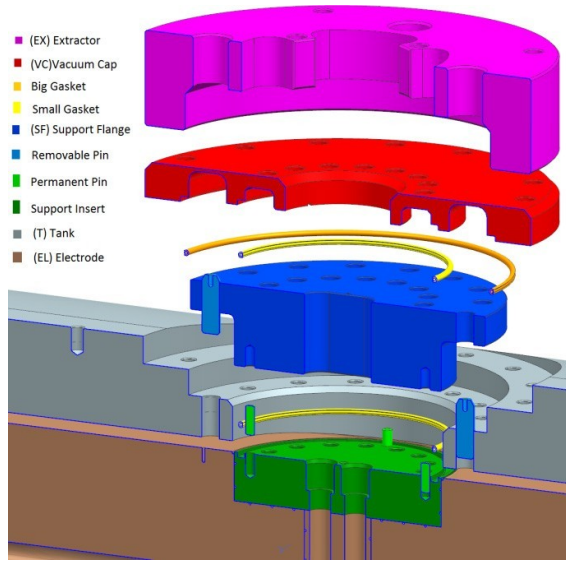


Figure 8: The assembly-alignment interface between electrodes and tank.

As for the inter-tank assembly, it has to be observed that slots for the bolt were added in order to increase the bending stiffness of the tank – tank interfaces and improve temperature uniformity. Moreover, calibrated shims will be bolted on a front face of a tank to obtain a correct relative positioning. Such shims could also be discontinuous to permit a He-leak test on the biggest seal of the cavity. As for tank positioning, no pins are used; relative positioning is made possible by the adjustable frame tools able to support any roll, pitch, and yaw effect of the inter tank planes (Fig. 9).

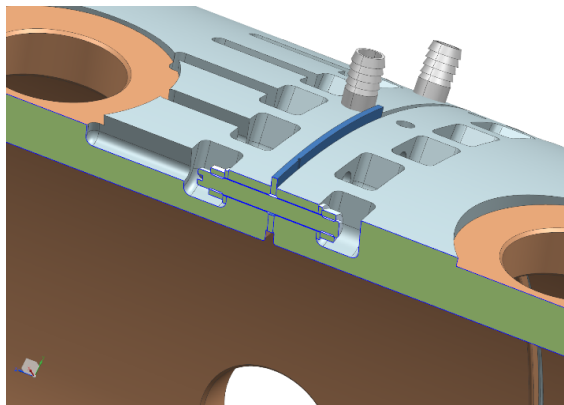


Figure 9: The inter-tank alignment detail: it is possible to recognise the slots for the bolts and the calibrated shims.

RFQ CONSTRUCTION AND TESTING

The construction of the electrodes (as well as tuners and vacuum grids) was done by CINEL Strumenti Scientifici s.r.l while the tanks were constructed by Fantini Sud Spa on the basis of design and drawings made at LNL; the Copperplating of the Tanks (copper thickness 70µm) was performed at CERN facilities. To date, all the electrodes and

tanks underwent complete construction and copper-plating. The first module to be assembled is module 5.

Despite to the electrodes with all the surfaces finished, the copper plated surfaces of the tank need to be re-finished with agate knife in order to avoid imperfections to obtain surfaces as smooth as possible, as experienced also in ESS [7]. Moreover, all the surfaces in contact with a vacuum gasket must be finished with a sandpaper with P320 grade to decrease the roughness and eliminate radial grooves due to the machining process. All tank surfaces were cleaned with isopropyl alcohol. After the re-finishing phase, metrological characterization of all the tank surfaces as well as the electrode surfaces was done in separate moments. A CMM arm 0.03 mm Maximum Permitted Error (MPE) with a ruby scanning probe was used. For all components a unique common coordinate system was defined. The superposition of the measured entities with the common reference system permits to obtain the ad-hoc geometry of Electrode/Tank interface components, i.e. the Support Flange (SF). The correct placement was determined by the CMM arm with respect to some common given reference surfaces. Module 5 has been assembled and passed all the tests (Fig. 10).

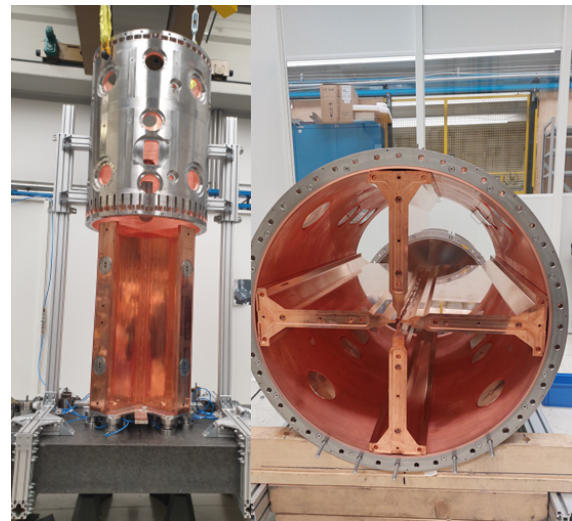


Figure 10: Initial positioning of Tank vs. electrodes (left), Final assembly of the RFQ module (right).

Tip positionings at the end faces of the module are within a range of ± 0.15 mm. Perpendicularity of the end faces of the module with respect to a representative beam axis, calculated using the tips deviations, are within 0.08 mm. Total tip deviations ΔR_0 at the middle plane of the module are about 0.02 mm. Vacuum test was carried out using the He spraying method. The pressure reached inside the chamber is about $1.2 \cdot 10^{-5}$ mbar and the maximum detected leak is about $3 \cdot 10^{-11}$ mbar-l/s].

A further validation step of the RFQ assembly procedure consists in RF measurements. In order to perform such characterization, the RFQ module is connected with a pair of hollow cylinders 0.5 m long each with the same diameter as the RFQ: the overall structure resonant frequencies are,

for electrode tips displacement in the order of ± 0.2 mm, in a linear relationship with the RFQ frequencies. Therefore it is possible to extrapolate the RFQ frequencies in these measurements for different electrode assemblies according to the relationship $f_{\text{QWG}} = c_1 * f_{\text{QRFO}} + c_0$, where f_{QWG} is the frequency of the Quadrupole mode of the RFQ connected with the cylinders, while f_{QRFO} is the frequency of the Quadrupole mode of the RFQ with perfect H boundary conditions at both ends. This setup is not optimized in terms of RF joints in cylinders, yet a Q_0 about 65% of the nominal value (for this particular configuration) was measured.

The measurements showed that, when assembled with nominal settings, the RFQ frequency only differs of 8 kHz from the simulated one and that, in three different alignment setups (#1: ruler checked alignment, no alignment pins, no machined flanges, no seals, #2: measuring arm checked alignment, alignment pins with 0.1 mm clearance, no seals, #3: measuring arm checked alignment, alignment pins with <0.05 mm clearance, seals installed), this difference decreases from +28 kHz (#1), to 18 kHz (#2), up to 8 kHz (#3). These measurements constitute a further validation of the RFQ alignment and assembly procedure.

As the testing and alignment procedure of the RFQ module is successfully established, it will be repeated for all the other RFQ modules. In particular, the next steps foresee the characterization of RFQ Module 4 and the intertank assembly and alignment.

RFQ ANCILLARIES

RFQ Support

The RFQ support and alignment frame was built by Fantini Sud srl upon LNL specifications and it is now installed in its final position. This support will also host the Solenoid immediately before the Low Energy End of the RFQ. After RFQ Module 5 was characterized, it was installed in its final position on the support (Fig. 11).



Figure 11: The Module 5 installed in its final position.

RF System

In an earlier phase of the project, it was thought to use a tetrode amplifier based on the 220 kW TH781 tube already

used for the IFMIF RFQ High Power Tests (175 MHz) nevertheless, due to some issues encountered in the availability of a commercial solution for a 200 kW 80 MHz cavity and the availability of MOSFETs with power capabilities in the order of 1.6–1.8 kW, it was decided to use a Solid State Amplifier with the same frequency and power, and the corresponding tendering is in phase of awarding. The SPES RFQ will make use of one coupler, based on the IFMIF RFQ design [8], and located approximately at halfway of the RFQ. In this case no circulator is foreseen, as the RF amplifier is rated to withstand up to 20% CW reflected power and full reflected power for 100 μ s. In order to compensate the dipole and quadrupole perturbations due to the presence of the loop, three tuners, located in the other RFQ quadrants at the same longitudinal position of the loop, are foreseen.

ACKNOWLEDGEMENTS

The authors wish to express their gratitude to the INFN Colleagues who took part to the achievements reached so far: Andrea Colombo (INFN-PD), Paolo Bottin and Riccardo Panizzolo (INFN-LNL) for their valuable contribution and help in all the RFQ assembly phase, and Enrico Fagotti (INFN-LNL) for fruitful discussion and encouragement.

REFERENCES

- [1] M. Comunian *et al.*, “Status of the SPES Exotic Beam Facility”, *J. Phys. Conf. Ser.*, vol. 1401, p. 012002, 2020.
doi:10.1088/1742-6596/1401/1/012002
- [2] M. Comunian, A. Palmieri, A. Pisent, and C. Roncolato, “The New RFQ as RIB Injector of the ALPI Linac”, in *Proc. IPAC’13*, Shanghai, China, May 2013, paper THPWO023, pp. 3812-3814.
- [3] L. Ferrari, A. Palmieri, and A. Pisent, “RF-Mechanical Design and Prototyping of the SPES RFQ”, in *Proc. IPAC’17*, Copenhagen, Denmark, May 2017, pp. 4166-4168.
doi:10.18429/JACoW-IPAC2017-THPIK033
- [4] A. Palmieri, INFN-LNL Annual Report 2015, https://www1.lnl.infn.it/~annrep/read_ar/2015/contributions/pdfs/207_G_105_G100.pdf
- [5] L. Ferrari, A. Palmieri, and A. Pisent, “Thermo-Mechanical Calculations for the SPES RFQ”, in *Proc. HIAT’15*, Yokohama, Japan, Sep. 2015, pp. 219-221.
doi:10.18429/JACoW-HIAT2015-WEPB13
- [6] E. Fagotti *et al.*, “Preparation and Installation of IFMIF-EVEDA RFQ at Rokkasho Site”, in *Proc. LINAC’16*, East Lansing, MI, USA, Sep. 2016, pp. 1005-1007.
doi:10.18429/JACoW-LINAC2016-THPLR066
- [7] P. Mereu *et al.*, “Details of the Manufacturing Processes of the ESS-DTL Components”, in *Proc. LINAC’18*, Beijing, China, Sep. 2018, pp. 260-263.
doi:10.18429/JACoW-LINAC2018-MOP0124
- [8] E. Fagotti *et al.*, “The Couplers for the IFMIF-EVEDA RFQ High Power Test Stand at LNL: Design, Construction and Operation”, in *Proc. LINAC’14*, Geneva, Switzerland, Aug.-Sep. 2014, paper TUPP093, pp. 643-645.